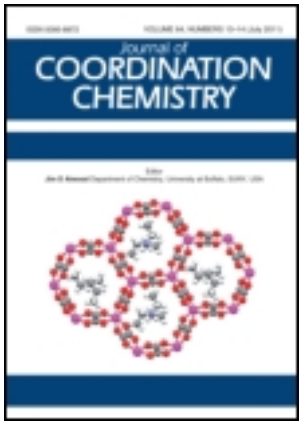

Journal of Coordination Chemistry
Publication details, including instructions for authors and subscription information:
http://www.tandfonline.com/loi/gcoo20

Dinuclear zinc(II) complexes with compartmental ligands: syntheses, structures, and bioactivities as artificial nuclease

Pali Maiti [a], Amitava Khan [b], Tanmay Chattopadhyay [c], Sudhanshu Das [a], Krishnendu Manna [b], Dipayan Bose [d], Sanjit Dey [b], Ennio Zangrando [e] & Debasis Das [a]

[a] Department of Chemistry, University of Calcutta, 92, A.P.C. Road, Kolkata - 700009, West Bengal, India

[b] Department of Physiology, University of Calcutta, 92, A.P.C. Road, Kolkata - 700009, West Bengal, India

[c] Department of Chemistry, Panchakot Mahavidyalya, Neturia, Purulia - 723121, West Bengal, India

[d] Cancer and Cell Biology Division, Indian Institute of Chemical Biology, 4, Raja S.C. Mullick Road, Kolkata - 70032, West Bengal, India

[e] Dipartimento di Scienze Chimiche e Farmaceutiche, University of Trieste, Via L. Giorgieri 1, 34127 Trieste, Italy

Published online: 04 Nov 2011.

To cite this article: Pali Maiti, Amitava Khan, Tanmay Chattopadhyay, Sudhanshu Das, Krishnendu Manna, Dipayan Bose, Sanjit Dey, Ennio Zangrando & Debasis Das (2011) Dinuclear zinc(II) complexes with compartmental ligands: syntheses, structures, and bioactivities as artificial nuclease, Journal of Coordination Chemistry, 64:21, 3817-3831, DOI: 10.1080/00958972.2011.631534

To link to this article: http://dx.doi.org/10.1080/00958972.2011.631534

Journal of Coordination Chemistry
Vol. 64, No. 21, 10 November 2011, 3817–3831

Dinuclear zinc(II) complexes with compartmental ligands: syntheses, structures, and bioactivities as artificial nuclease

PALI MAITI†, AMITAVA KHAN‡, TANMAY CHATTOPADHYAY§, SUDHANSHU DAS†, KRISHNENDU MANNA‡, DIPAYAN BOSE¶, SANJIT DEY‡, ENNIO ZANGRANDO†‡§¶ and DEBASIS DAS*†

†Department of Chemistry, University of Calcutta, 92, A.P.C. Road, Kolkata – 700009, West Bengal, India
‡Department of Physiology, University of Calcutta, 92, A.P.C. Road, Kolkata – 700009, West Bengal, India
§Department of Chemistry, Panchakot Mahavidyalya, Neturia, Purulia – 723121, West Bengal, India
¶Cancer and Cell Biology Division, Indian Institute of Chemical Biology, 4, Raja S.C. Mullick Road, Kolkata – 70032, West Bengal, India
†‡§¶Dipartimento di Scienze Chimiche e Farmaceutiche, University of Trieste, Via L. Giorgieri 1, 34127 Trieste, Italy

(*Received 6 July 2011; in final form 28 September 2011*)

Four water-soluble dinuclear Zn(II) complexes (**1**–**4**) of compartmental ligand L = 2,6-bis(R-iminomethyl)-4-R′-phenolate (where R = N-ethylpiperidine or R = N-ethylpyrrolidine, R′ = methyl or *tert*-butyl) have been synthesized, characterized, and their DNA cleavage activity and cytotoxicity toward HepG2 cancerous cells are evaluated. The dinuclear complexes are formed by a pentadentate-substituted phenolate ligand chelating the metal ions separated by *ca* 3.27 Å. Each metal is a distorted trigonal bipyramid, completing the coordination sphere through acetate. The X-ray structural determination of **2** shows that the complex is counterbalanced by half $Zn(SCN)_4^{2-}$ (formulation $[Zn_2L^2(CH_3CO_2)_2][(Zn(SCN)_4]_{0.5}$), while in **1** and **3** two crystallographically-independent complexes are present in the unit cell with a $Zn(SCN)_4^{2-}$. Among the four complexes only the 4-*tert*-butyl-phenolato derivatives (**3** and **4**) show DNA cleavage activity in *in-vivo* conditions and appear to be promising toward metal complexes to be used as anticancer agents. The cytotoxicity of the complexes, investigated through MTT assay, suggests that **4** is a better choice as artificial nuclease.

Keywords: Schiff-bases; Zinc complexes; Compartmental ligands; DNA cleavage; cytotoxicity

1. Introduction

Bioinorganic chemists use small molecule models to understand the functional mechanisms of metallobiosites with the ultimate goal to apply the knowledge acquired to develop systems to serve mankind. Design and synthesis of model compounds having potential to bind and cleave DNA, the heart of cellular translation and transcription is

*Corresponding author. Email: dasdebasis2001@yahoo.com

ISSN 0095-8972 print/ISSN 1029-0389 online © 2011 Taylor & Francis
http://dx.doi.org/10.1080/00958972.2011.631534

a part of the goal. Lewis acidic metal centers are chemically suited to induce fundamental cellular processes for their ability to coordinate nitrogen and oxygen donors, as well as to their aptitude to support larger aromatic architectures capable of π interactions with the nucleic acid building blocks. Zinc(II) is the best choice as Lewis acid to perform various biological functions. The role and behavior of zinc in all such bioinorganic processes are modulated by its coordination environment, where Zn^{II} can be four-, five-, or six-coordinate. In enzymes the coordination number for Zn^{II}, usually smaller than six, provides available binding sites in the metal coordination sphere. Interaction with DNA duplex generally occurs by three different binding modes, intercalation [1], covalent binding [2], and non-covalent binding [3, 4] (electrostatic, groove binding, and hydrogen binding). DNA binding and/or cleavage by small coordination complexes received new impetus recently since most chemotherapeutic anticancer agents currently used target DNA [5, 6]. Although many mononuclear complexes of Schiff-base, diamine, azacrown, and aminocarboxylate ligands are effective [7–10], the recent trend is to develop dinuclear and multinuclear metal assemblies that better position metal ions at the cleavage site and enhance DNA cleavage activity [11–13]. We have prepared four dinuclear zinc(II) complexes of general formula $[Zn_2L^{1-4}(OAc)_2]_2[Zn(SCN)_4]$ [where L is the compartmental ligand 2,6-bis(R-iminomethyl)-4-methyl-phenolate (L^{1-2}) or 2,6-bis(R-iminomethyl)-4-*tert*-butyl-phenolato (L^{3-4}), where R is N-ethylpiperidine or N-ethylpyrrolidine), see scheme 1]. The effectiveness of these complexes to bind and cleave supercoiled (SC) plasmid DNA, the cleavage mechanism, and the cytotoxicity on human cancer cell line have been investigated.

2. Experimental

2.1. *Materials and methods*

All chemicals were obtained from commercial sources and used as received. Solvents were dried according to the standard procedure and distilled prior to use. 4-Methyl-2,6-diformylphenol and 4-*tert*-butyl-2,6-diformylphenol were prepared according to the

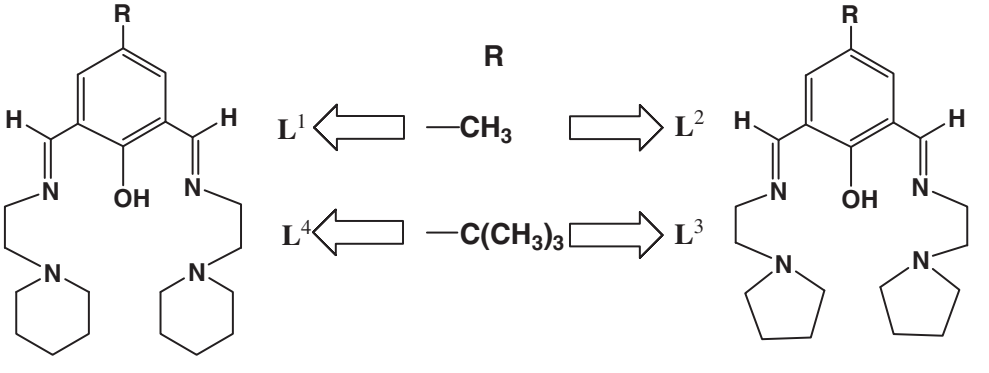

Scheme 1. Chemical drawing of the compartmental ligands.

literature method [14]. *N*-(2-aminoethyl)piperidine, *N*-(2-aminoethyl)pyrrolidine, and zinc(II) acetate were purchased from Aldrich Chemical Company and used as received. All other chemicals were of AR grade. Elemental analyses (carbon, hydrogen, and nitrogen) were performed using a Perkin-Elmer 240C elemental analyzer. Infrared spectra (4000–400 cm^{-1}) were recorded at 25°C using a Shimadzu UV-3101PC where KBr was used as medium. Electronic spectra (200–1600 nm) were obtained at 25°C using a Shimadzu UV-3101PC where dry acetonitrile/dry methanol/nujol were used as medium as well as reference. Fluorescence spectra of the complexes with varying amounts of DNA in aqueous medium were recorded with a Perkin–Elmer model LS 55 Luminescence Spectrometer.

2.2. *Syntheses of complexes*

2.2.1. $[Zn_2L^1(OAc)_2]_2[Zn(SCN)_4]$ (1). A methanolic solution (5 mL) of *N*-(2-aminoethyl)piperidine (0.2564 g, 2 mmol) was added dropwise to a hot methanolic (10 mL) solution of 4-methyl-2,6-diformylphenol (0.164 g, 1 mmol) and the resulting mixture was refluxed for half an hour. Then, a methanolic solution (10 mL) of Zn-acetate (0.439 g, 2 mmol) was added under continuous stirring. After 2 h, a water solution (5 mL) of sodium thiocyanate (0.2026 g, 2.5 mmol) was added to the yellow solution followed by stirring for 8 h. The resulting yellow solution was then kept in a $CaCl_2$ desiccator in the dark, and square-shaped light yellow crystals were obtained after a few days. (Yield 72%). Anal. Calcd for $C_{58}H_{82}N_{12}O_{10}S_4Zn_5$ (%): C, 44.59; H, 5.29; N, 10.76; Found (%): C, 44.51; H, 5.22; N, 10.69; IR: ν(C=N) 1644 cm^{-1}; ν(skeletal vibration) 1587 cm^{-1}; $\nu(H_2O)$ 3431 cm^{-1}; $\nu(SCN^{-1})$ 2069 cm^{-1}. UV(MeOH) (nm^{-1}): 393 ($\varepsilon = 7365$ $(mmol)^{-1}$ cm^{-1}).

2.2.2. $[Zn_2L^2(OAc)_2]_2[Zn(SCN)_4]$ (2). Complex **2** was prepared similar to **1** by using *N*-(2-aminoethyl)pyrrolidine (0.2284 g, 2 mmol) instead of *N*-(2-aminoethyl)piperidine. (Yield 70%). Anal. Calcd for $C_{27}H_{37}N_6O_5S_2Zn_5$ (%): C, 43.05; H, 4.95; N, 11.15; Found (%): C, 42.93; H, 4.87; N, 11.09; IR: ν(C=N) 1645 cm^{-1}; ν(skeletal vibration) 1549 cm^{-1}; $\nu(H_2O)$ 3432 cm^{-1}; $\nu(SCN^{-1})$ 2074 cm^{-1}. UV(MeOH) (nm^{-1}): 391 ($\varepsilon = 6414$ $(mmol)^{-1}$ cm^{-1}).

2.2.3. $[Zn_2L^3(OAc)_2]_2[Zn(SCN)_4]$ (3). Complex **3** was prepared following a similar procedure to that for **1** by reacting *N*-(2-aminoethyl)pyrrolidine (0.2284 g, 2 mmol) with 4-*tert*-butyl-2,6-diformylphenol (Yield 70%). Anal. Calcd for $C_{50}H_{78}N_{12}O_{10}S_4Zn_5$ (%): C, 45.14; H, 4.67; N, 10.53; Found (%): C, 45.07; H, 4.59; N, 10.47; IR: ν(C=N) 1645 cm^{-1}; ν(skeletal vibration) 1594 cm^{-1}; $\nu(H_2O)$ 3449 cm^{-1}; $\nu(SCN^{-1})$ 2073 cm^{-1}. UV(MeOH) (nm^{-1}): 387 ($\varepsilon = 17149$ $(mmol)^{-1}$ cm^{-1}).

2.2.4. $[Zn_2L^4(OAc)_2]_2[Zn(SCN)_4]$ (4). Complex **4** was prepared similar to **3** by using *N*-(2-aminoethyl)piperidine (0.2284 g, 2 mmol) instead of *N*-(2-aminoethyl)pyrrolidine. (Yield 70%). Anal. Calcd for $C_{50}H_{78}N_{12}O_{10}S_4Zn_5$ (%): C, 46.39; H, 5.72; N, 10.15; Found (%): C, 46.32; H, 5.68; N, 10.08; IR: ν(C=N) 1643 cm^{-1}; ν(skeletal vibration)

1593 cm^{-1}; $\nu(H_2O)$ 3436 cm^{-1}; $\nu(SCN^{-1})$ 2073 cm^{-1}. UV(MeOH) (nm^{-1}): 391 ($\varepsilon = 19019$ $(mmol)^{-1}\,cm^{-1}$).

2.3. *X-ray data collection and crystal structure determination*

Diffraction data for **1** and **2** were collected on a Nonius DIP-1030H system and for **3** on a BRUKER SMART APEX diffractometer equipped with a CCD detector. All experiments were performed at room temperature with Mo-Kα radiation ($\lambda = 0.71073$ Å). Cell refinement, indexing, and scaling of the data set were carried out using Denzo [15], Scalepack [16], Bruker Smart Apex, and Bruker Saint packages [17]. The structures were solved by direct methods and subsequent Fourier analyses and refined by full-matrix least-squares based on F^2 with all the observed reflections [18]. Hydrogen atoms, generated by SHELXL [18] at calculated positions, were introduced in the final cycles of refinement. A piperidine ring in **1** has a methylene disordered over two positions, corresponding to a boat and a chair conformation of the ring (occupancy of 0.50). A *t*-butyl group of **3** was disordered over two orientations of methyl groups (occupancies of 0.58/0.42). Crystallographic data and details of refinements are reported in table 1. All calculations were performed using the WinGX System, Ver 1.80.05 [18].

2.4. *Bioactivity*

Human hepatocellular carcinoma cells (Hep G2) were cultured [19, 20] as a monolayer, grown in a suspension in the complete nutrient medium, at 37°C in humidified air with 5% CO_2. Hep G2 cells (2×10^5 per well) were seeded into 96-well microtiter plates. Twenty-four hours later, after cell adherence, complexes at six different concentrations were added to the wells, except for the control cells to which only a nutrient medium was added. Nutrient medium was RPMI-1640, supplemented with l-glutamine (3 mM), streptomycin (100 lg mL^{-1}), and penicillin (100 IU mL^{-1}), 10% heat inactivated (56°C) FBS and 25 mM Hepes, and the pH of the medium was adjusted to 7.2 by bicarbonate solution. The assay was performed as follows: 20 μL of MTT solution (3-(4,5-dimethylthiazol-2-yl)-2,5-diphenyltetrazolium bromide, 5 mg mL^{-1} in phosphate buffered saline) were added to each well and the samples were incubated for further 4 h. Then, 100 μL of 10% SDS was added to extract the insoluble product formazan, resulting from the conversion of the MTT dye by viable cells. The number of viable cells in each well was proportional to the light absorbance, which was determined in an ELISA plate reader at 595 nm.

3. Results and discussion

Active sites of metallo-enzymes have been modeled by using compartmental ligands having an endogenous bridging phenolate. The efficiency of such systems to form dinuclear complexes and their capability to stabilize the dinuclear frameworks have already been validated by several groups including our laboratory [21, 22]. As extension of our previous works in this field, we designed dinuclear Zn complexes by adopting

Table 1. Crystal data and details of structure refinements for **1–3**.

	1	**2**	**3**
Empirical formula	$C_{58}H_{82}N_{12}O_{10}S_4Zn_5$	$C_{27}H_{37}N_6O_5S_2Zn_{2.50}$	$C_{60}H_{86}N_{12}O_{10}S_4Zn_5$
Formula weight	1562.45	753.17	1590.50
Crystal system	Monoclinic	Monoclinic	Monoclinic
Space group	$P2_1/c$	$C2/c$	$C2/c$
Unit cell dimensions (Å, °)			
a	11.623(3)	34.162(6)	37.801(3)
b	47.578(6)	8.705(2)	13.1093(9)
c	13.640(3)	22.941(3)	30.264(2)
β	107.46(3)	101.249(2)	94.329(2)
Volume (Å^3), Z	7195(3), 4	6691(2), 8	14954.1(18), 8
Calculated density (g cm^{-3})	1.442	1.495	1.413
Absorption coefficient (mm^{-1})	1.818	1.952	1.751
$F(000)$	3232	3104	6592
θ_{max} (°)	23.26	26.37	27.48
Reflections collected	71,738	47,688	107,217
Independent reflection	9760 [R(int) = 0.0720]	6378 [R(int) = 0.0616]	16,976 [R(int) = 0.1016]
Observed [$I > 2\sigma(I)$]	3271	3502	8000
Parameters	526	386	851
Goodness-of-fit on (F^2)	0.876	0.871	1.008
Final R indices [$I > 2\sigma(I)$] [a]	$R_1 = 0.0675$, $wR_2 = 0.1876$	$R_1 = 0.0443$, $wR_2 = 0.1068$	$R_1 = 0.0580$, $wR_2 = 0.1436$
Largest difference peak and hole (e Å^{-3})	0.616, −0.346	0.590, −0.263	0.728, −0.424

[a] $R_1 = \Sigma\|F_o| - |F_c\| \,/\, \Sigma|F_o|$, $wR_2 = [\Sigma w(F_o^2 - F_c^2)^2 \,/\, \Sigma w(F_o^2)^2]^{1/2}$.

a template synthesis that requires 2,6-diformyl-4-methylphenol, 4-*tert*-butyl-2,6-diformylphenol, *N*-(2-aminoethyl)piperidine, *N*-(2-aminoethyl)pirrolidine, zinc(II) acetate, and sodium thiocyanate. IR spectra of all the complexes show bands at 1643–1647 cm^{-1} due to C=N stretch and 1549–1594 cm^{-1} for skeletal vibration. The band at 1420–1446 cm^{-1} is attributed to symmetric bridging carboxylate; the asymmetric bridging carboxylate is most likely merged with the skeletal vibration. A very strong band at 2066–2075 cm^{-1} can be attributed to monodentate thiocyanate.

3.1. *Description of crystal structures*

The RX structural analyses of **1–3** confirm the formation of dinuclear complex cations. For **2** the complex is counterbalanced by half $Zn(SCN)_4^{2-}$ located on a two-fold axis (complex formulation $[Zn_2L^2(CH_3CO_2)_2][(Zn(SCN)_4]_{0.5}$), while in **1** and **3** two crystallographically independent complexes are present in the unit cell with a $Zn(SCN)_4^{2-}$. The dinuclear complexes are formed by a pentadentate phenolate chelating the metal. Each Zn is five coordinate, distorted trigonal bipyramid with a bridging phenoxy oxygen, two N-donors (from the imine and amine donors), and two oxygen atoms from acetate bridging anions. ORTEP views with atom labeling of **1–3** are shown in figures 1–3, and a selection of bond lengths and angles is given in table 2. Making allowance for the e.s.d.'s, the coordination distances are comparable in all the complexes. The Zn–O(phenoxy) bond distances from 2.080(3) to 2.123(3) Å are slightly longer than the Zn–O(acetate) ones that fall between 1.927(8) and 2.021(10) Å (mean value of 1.963 Å). The values measured for Zn–N(amino), relative to the side

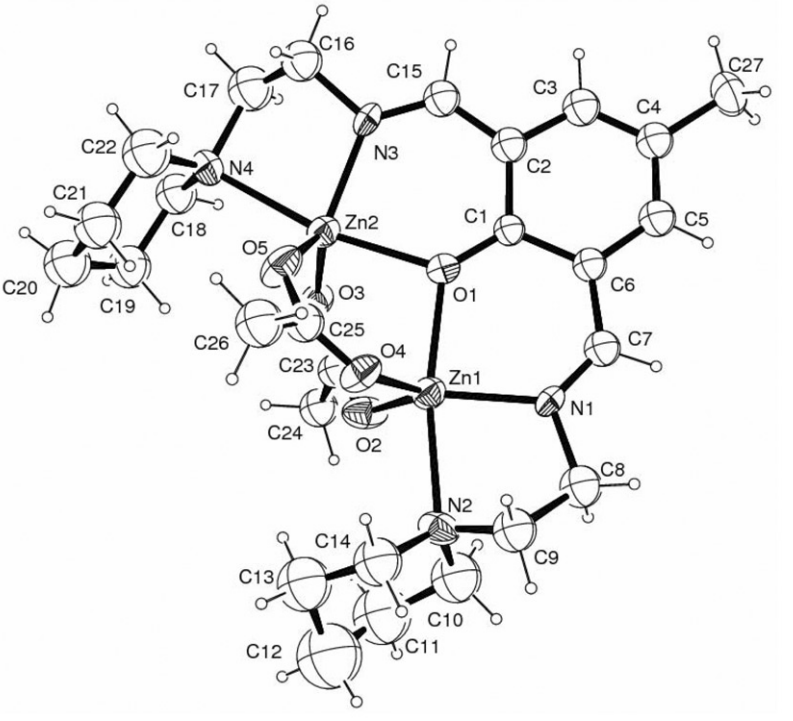

Figure 1. ORTEP view of the complex cation A of **1**.

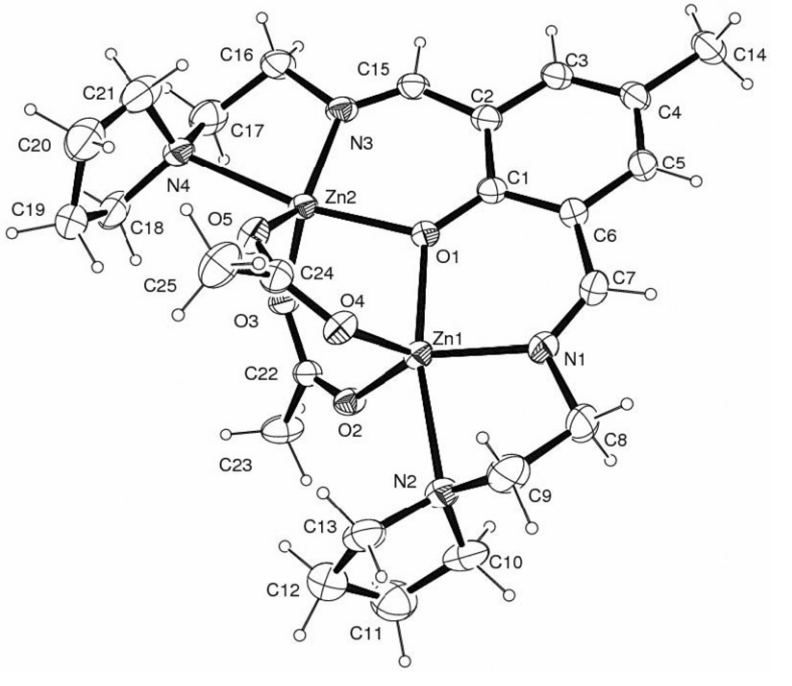

Figure 2. ORTEP view of the complex cation of **2**.

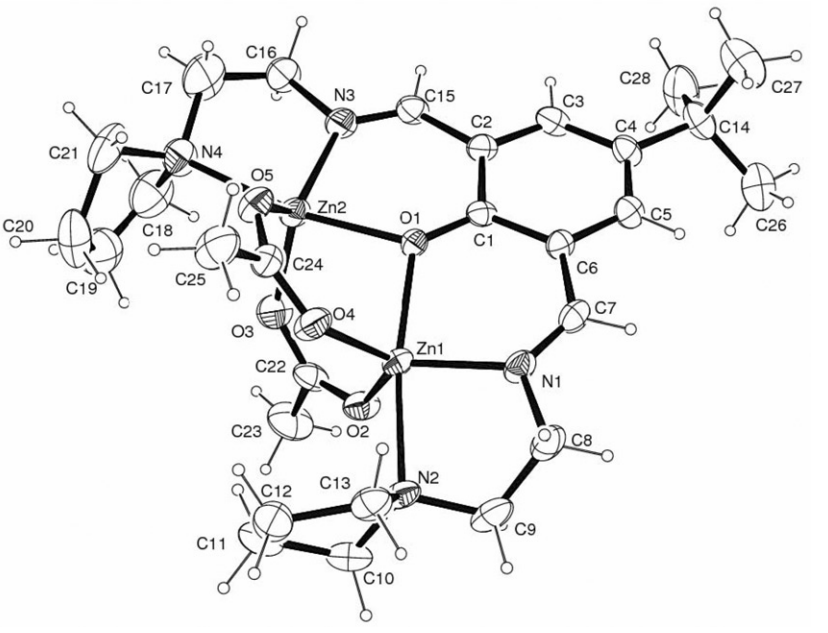

Figure 3. ORTEP view of the complex cation A of **3**.

Table 2. Selected bond lengths (Å) and angles (°) for **1–3**.

	1			**3**	
	Complex A	Complex B[a]	**2**	Complex A	Complex B[a]
Zn(1)–N(1)	1.992(12)	2.028(10)	1.996(4)	2.005(4)	1.984(5)
Zn(1)–O(1)	2.113(8)	2.095(8)	2.097(2)	2.123(3)	2.100(4)
Zn(1)–N(2)	2.270(9)	2.489(14)	2.330(3)	2.235(4)	2.249(5)
Zn(1)–O(2)	1.927(8)	1.959(7)	1.965(3)	1.959(4)	1.948(5)
Zn(1)–O(4)	1.967(8)	1.945(7)	1.987(3)	1.958(4)	1.950(5)
Zn(2)–N(3)	2.023(12)	2.015(10)	2.017(3)	2.010(4)	2.006(6)
Zn(2)–O(1)	2.114(9)	2.086(6)	2.080(3)	2.123(3)	2.097(4)
Zn(2)–N(4)	2.329(11)	2.234(8)	2.313(3)	2.223(4)	2.252(6)
Zn(2)–O(3)	1.965(7)	2.021(10)	1.992(2)	1.952(4)	1.939(5)
Zn(2)–O(5)	1.948(8)	1.976(7)	1.965(3)	1.954(4)	1.976(5)
Zn–Zn	3.286(2)	3.270(2)	3.2749(7)	3.2386(9)	3.2807(8)
d(Zn)[a]	0.102(8)	0.722(8)	0.232(3)	0.432(4)	0.006(3)
	0.327(8)	−0.185(8)	−0.133(3)	0.113(5)	−0.260(6)
O(2)–Zn(1)–O(4)	112.6(4)	122.9(3)	106.84(12)	119.1(2)	115.74(18)
O(2)–Zn(1)–N(1)	126.6(4)	125.3(3)	138.49(14)	119.0(2)	114.41(18)
O(4)–Zn(1)–N(1)	120.4(4)	111.6(3)	113.10(14)	121.6(2)	129.32(19)
O(1)–Zn(1)–N(2)	168.8(4)	168.8(3)	168.11(12)	170.75(19)	168.91(15)
O(5)–Zn(2)–O(3)	121.1(4)	105.9(4)	106.50(12)	116.9(2)	115.15(17)
O(3)–Zn(2)–N(3)	122.0(4)	105.4(4)	113.08(13)	117.4(3)	120.13(19)
O(5)–Zn(2)–N(3)	116.9(4)	148.4(4)	139.00(13)	125.5(2)	124.43(19)
O(1)–Zn(2)–N(4)	167.4(4)	171.1(4)	168.68(11)	168.8(2)	167.67(15)
Zn–O(1)–Zn	102.1(4)	102.9(3)	103.27(11)	101.03(17)	101.18(13)
Ac/Ac[c]	49(1)	52.5(6)	60.1(2)	52.2(4)	71.4(3)

[a]In **1** and **3** atom labels for the complexes A and B follow a similar order.
[b]*d*(Zn) = displacement of Zn ions from the phenolate mean plane.
[c]Dihedral angle between acetate mean planes.

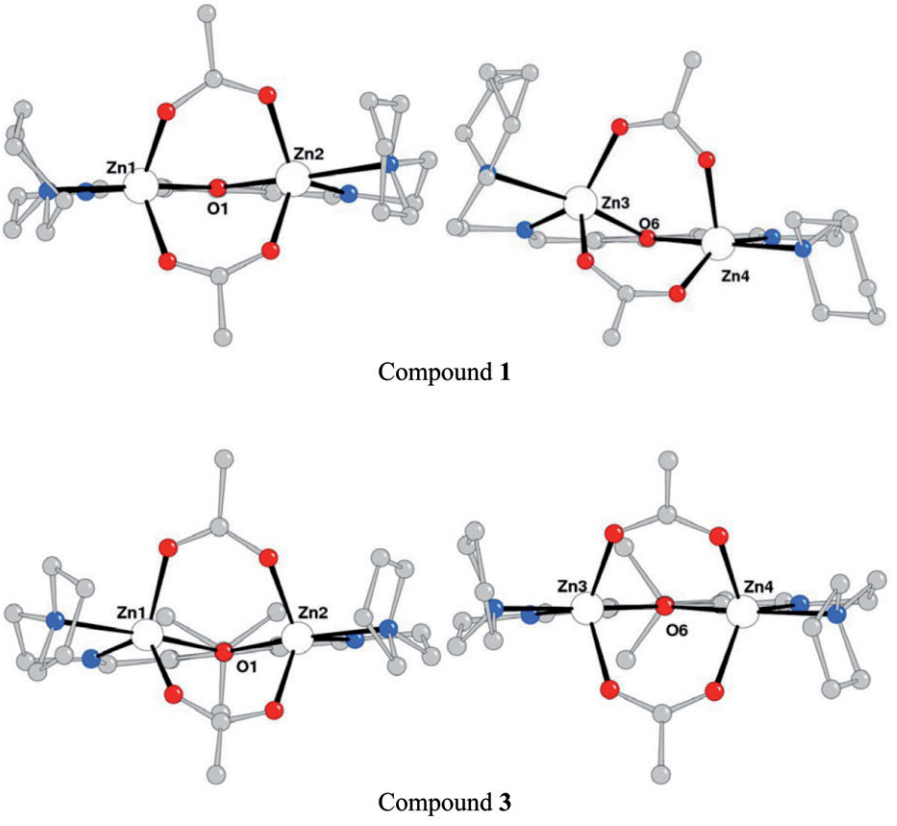

Figure 4. Perspective view of the two independent complexes A and B in **1** and **3** highlighting the displacement of Zn from the phenolate mean plane.

cyclic amine rings (range 2.223(4)–2.489(14) Å), are considerably longer than the Zn–N(imino) bond length averaging to 2.008 Å, revealing a labile bond between the piperidine and pyrrolidine donor and zinc. The different hybridized N donor type does not explain this feature that appears to arise from steric reasons. It is evident from data of table 2 that substitution of methyl by a *t*-butyl in the phenolate ring of **3** does not influence the coordination bond distances, although an electronic effect would be expected. The O(phenoxy) and N(amino) donors, in axial positions in the trigonal bipyramidal geometry, have an O–Zn–N bond angle of *ca* 169°. O(acetate)–Zn(1)–N(1) and O(acetate)–Zn(2)–N(3) angles in the equatorial plane deviate significantly from the ideal values of 120°, as observed in the coordination sphere of complex B in **1**, where these values fall between 105.4(4) and 148.4(4)°. The distortions in coordination bond angles (especially in **1** and **2**) seem to be provoked by the presence of a sulfur (of the anion) at short distance from zinc (S···Zn4 = 3.44 Å in complex B of **1**, two interactions of mean distance 3.80 Å in **2**). Conformational distortions of the complexes are shown by the displacement of zinc from the phenolate mean plane (up to 0.7 Å) and by the acetate bridging fragments, the mean planes of which form dihedral angles that vary from 50° to 70°. The perspective view of the two independent complexes A and B in **1** and **3** (figure 4) is indicative of conformational freedom in solution. The Zn–Zn

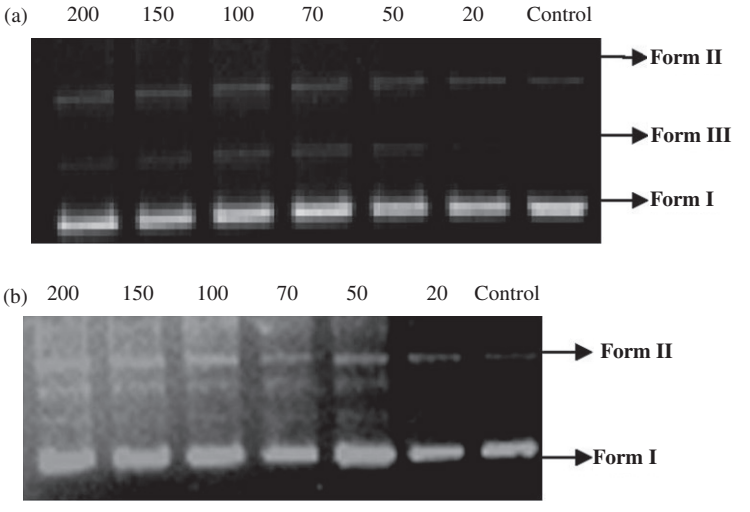

Figure 5. Gel electrophoresis showing the cleavage of SC pET28a plasmid DNA (300 ng in each lane) with different concentrations of (a) **3** and (b) **4** in the presence of 10 mM Tris EDTA buffer (pH 7.0) at 37°C for 45 min.

separations, mean value of 3.270 Å, are slightly longer than those usually found in Zn containing Robson-type [23] macrocycles (*ca* 3.1 Å).

The complex anions have a distorted tetrahedral geometry with SCN binding Zn through nitrogen (Zn–N bond distances range from 1.922(12) to 1.972(7) Å, N–Zn–N angles range from 104.0(3) to 114.8(5)°). The thiocyanates are not linear, but bent, with the largest divergence for a Zn–N–C angle in the anion of **1**, 152.6(14)°.

The structural features may have significant implications in the biological activity of these complexes. Although single crystals for **4** have not been obtained, we may anticipate a molecular structure similar to those reported here.

3.2. *DNA cleavage activity*

DNA cleavage ability of **1**–**4** was assessed by investigating their activity with SC pET28a plasmid DNA and for this purpose the SC DNA (300 ng for each set) was incubated with each complex at different concentrations in the presence of 10 mM Tris buffer (pH 7) at 37°C for 45 min. The reaction was stopped with 1X DNA loading dye and resolved in 1% agarose gel. Upon gel electrophoresis of the reaction mixture, a concentration-dependent DNA cleavage was noticed for **3** and **4** (figure 5a and 5b, respectively), but no activity was observed with **1** and **2**.

The band intensity of SC, nicked circular (NC) and linear (L) forms was measured through densitometric analysis (BIORAD QUANTITY ONE software) and plotted against increasing concentration of the complex (figure 6a and 6b). Complexes **3** and **4** exhibit DNA cleavage in different degrees and, as far as DNA breaking efficiency is concerned, **4** shows superior activity. However, densitometric analysis data show that these complexes can cause SC DNA cleavage even at a concentration of 20 μM.

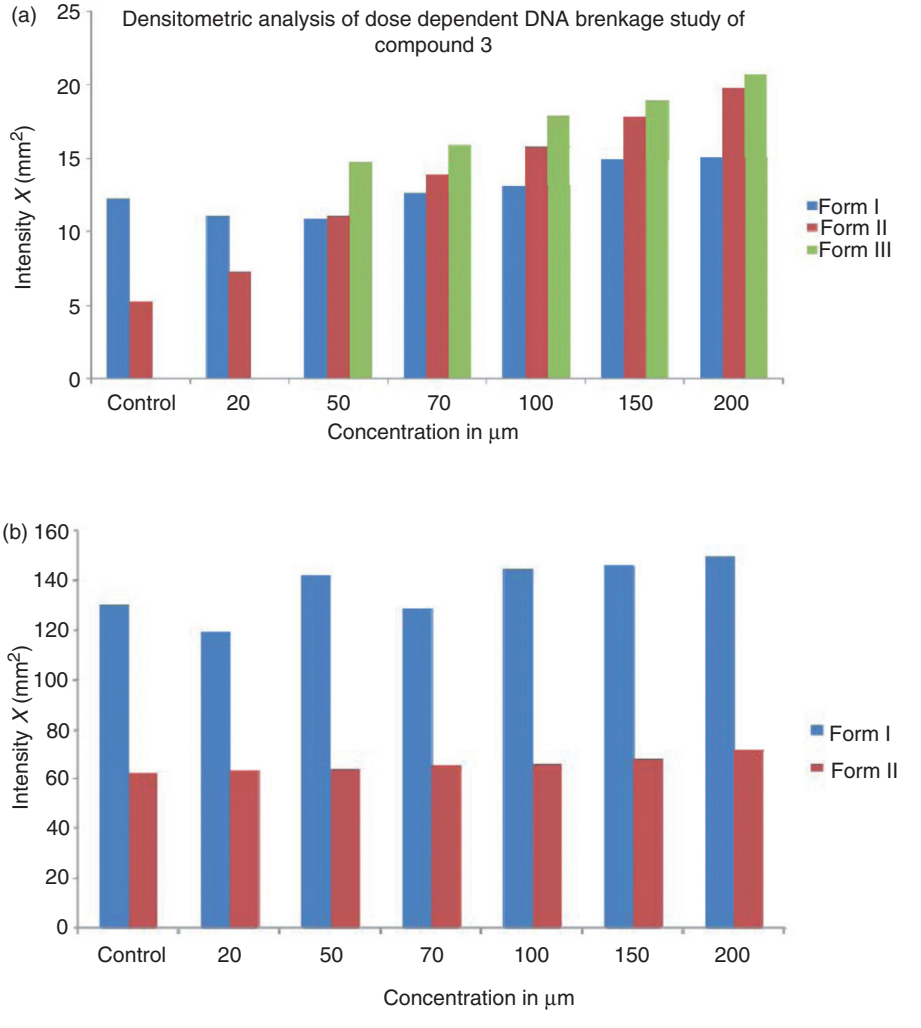

Figure 6. Relative amounts of different DNA forms with increasing concentration of (a) **3** and (b) **4** by densitometric analysis; SC indicated in blue; NC in red; L in green for (a).

Though we obtained robust formation of NC and L by increasing the concentration of **3** and **4**, we did not find proportionate decrease in SC in gel or densitometric scans. This might be due to auto fluorescence of these complexes or along with their intercalation with DNA as intermediate complex in the gel when visualized through UV at 254 nm. Reports on DNA cleavage by zinc(II) complexes are limited. The results reveal that two mechanisms are likely involved in DNA cleavage: (i) hydrolytic cleavage and (ii) free radical mechanism. The DNA cleavage by **3** and **4** is inhibited to a significant extent when the reaction is carried out in the presence of DMSO (above 50 µM), which is a hydroxyl radical scavenger, but not in the presence of even high concentration of NaN_3 (figure 7 for **4** as representative), which may act as a singlet oxygen scavenger. These data suggest that both complexes are cleaving artificial

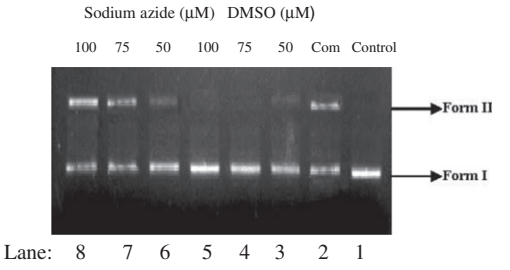

Figure 7. Lane 1: pET28a plasmid DNA (300 μg in lane). Lane 2: pET28a plasmid DNA (300 ng in lane) with 200 μM of **4** alone. Lanes 3–5: pET28a plasmid DNA (300 ng in lane) with 200 μM of **4** in the presence of radical scavenger DMSO. Lanes 6–8: pET28a plasmid DNA (300 ng in lane) with 200 μM of **4** in the presence of NaN3.

nucleases via hydroxyl radical pathway. Complexes **3** and **4** are fluorescent and their fluorescence intensity is enhanced in the presence of DNA (figure 8a, 8b). We have exploited this phenomenon to determine the intrinsic DNA binding constant by applying Benesi–Hildebrand model [24] (figure 9a, 9b), allowing the estimation of K_{intr} for **3** and **4** as 6.7×10^4 and $5.26 \times 10^4\,(\text{mmol})^{-1}$, respectively.

3.3. *Bio-activity*

The cytotoxicity of **1**–**4** towards HepG2 cancer cells was determined by MTT assay after incubation of the treated cells for 72 h and different behavior was observed. Complexes **2** and **4** are more cytotoxic towards the HepG2 cell line (figure 10) with about 50% cells viable at 30 μM dose, whereas **1** and **3** are not cytotoxic even at 75 μM. The cell death rate (%) is evaluated as

$$\frac{(\text{OD of control group} - \text{OD of treated group})}{(\text{OD of control group})} \times 100$$

where OD was measured at 595 nm. The apparently high dose (30 μM) may be compared with earlier reports [21, 22, 25] for similar systems.

4. Conclusions

Four dinuclear zinc(II) complexes of phenol-based compartmental ligands 2,6-bis(R-iminomethyl)-4-R'-phenolato (where R = N-ethylpiperidine or R = N-ethylpyrrolidine, R' = methyl or *tert*-butyl) have been synthesized and characterized with three structures by single-crystal X-ray analyses. The structural analyses reveal comparable configurations, although with distortions in the metal coordination sphere and the presence of short contacts between sulfur of $[Zn(SCN)_4]^{2-}$ and the dinuclear zinc(II) complexes. DNA cleavage and cytotoxicity toward hepatocellular carcinoma cells by all four complexes have been investigated to understand their viability as artificial nucleases and thereby their possible role as anticancerous agents.

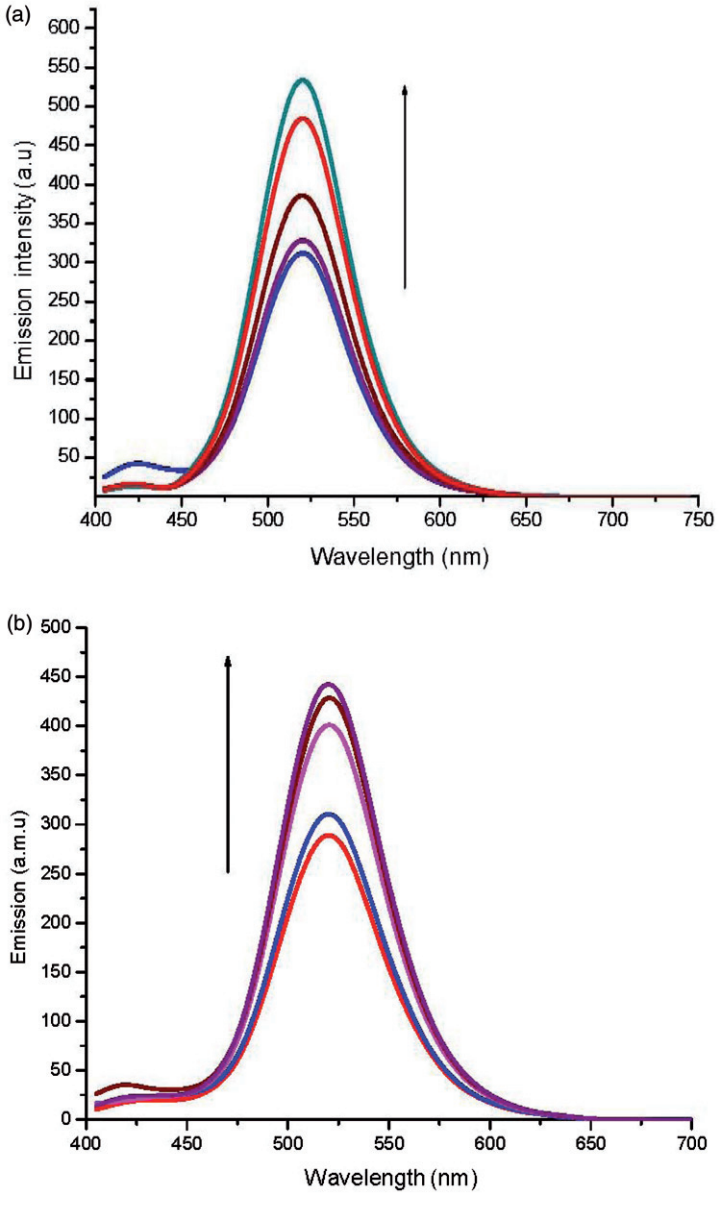

Figure 8. Emission spectra of (a) 3 and (b) **4** in 10 mM Tris-HCl (pH 7) buffer in the absence and presence of increasing amounts of DNA (μM).

Complexes with 4-methyl-phenolato (**1**, **2**) are inactive toward DNA cleavage, whereas complexes with 4-*tert*-butyl-phenolato (**3**, **4**) are highly active with **4** showing the largest effect. Since **3** and **4** bind and cleave DNA by a self-activating mechanism, probably via hydroxyl radical pathway, their application in site-specific recognition of DNA even in *in-vivo* conditions is promising. MTT assay suggests that **4** is a better choice as artificial

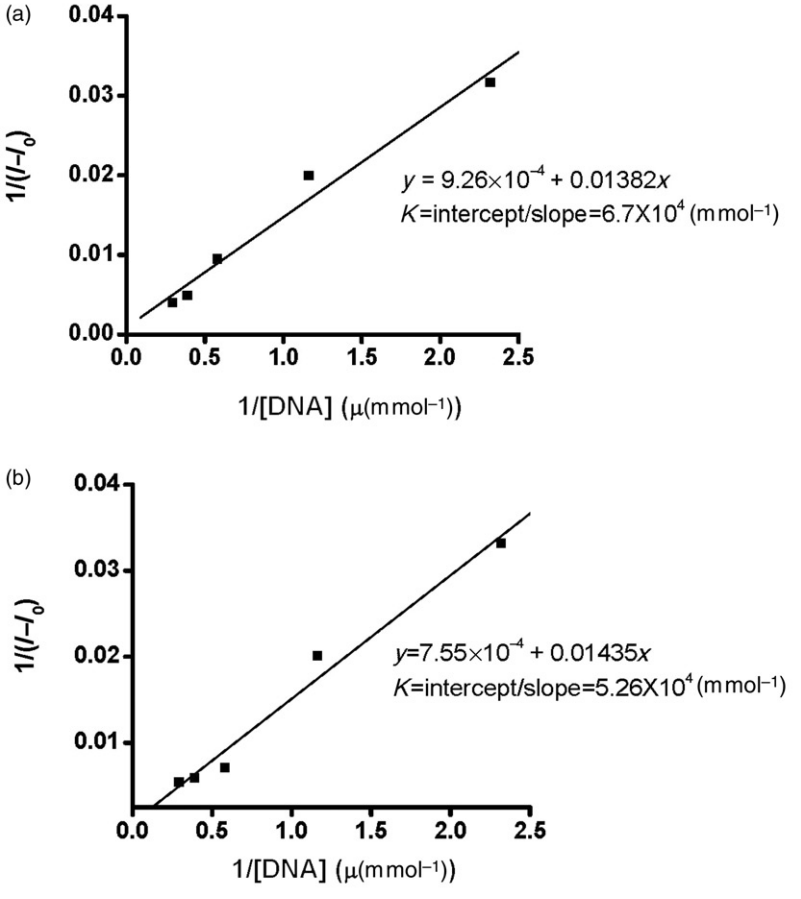

Figure 9. Benesi-Hildebrand plot of (a) **3** and (b) **4**.

nuclease with anti-proliferating effect on cancerous cell and this behavior may be important along with its water solubility, for applications in site-specific recognition of DNA, as well as for a promising anticancer drug.

Supplementary material

Crystallographic data (excluding structure factors) has been deposited with the Cambridge Crystallographic Data Centre as supplementary publication CCDC 818832–818834 for **1**–**3**. Copies of the data can be obtained free of charge on application to CCDC, 12 Union Road, Cambridge CB2 1EZ, UK (Email: deposit@ccdc.cam.ac.uk).

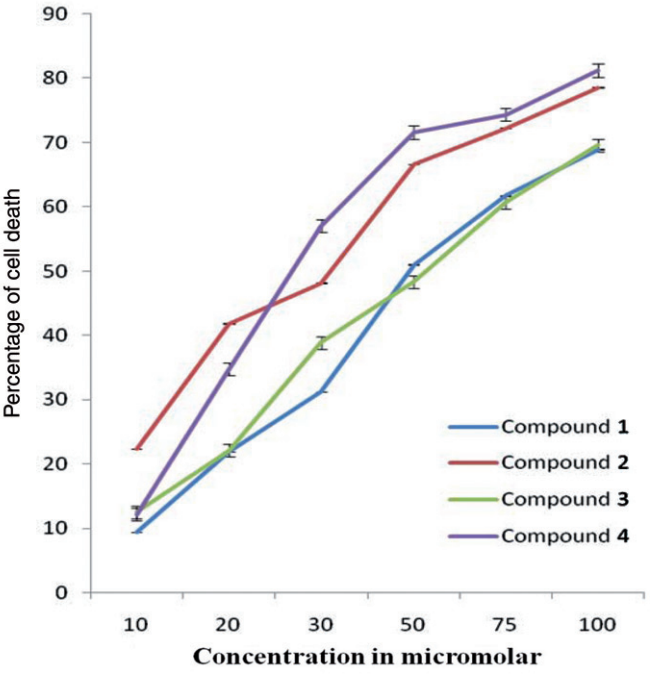

Figure 10. Hep G2 cells inhibition by **1–4** estimated by MTT assay. Data are expressed as percentage of cell death with respect to untreated controls.

Acknowledgments

The authors wish to thank the University Grants Commission, New Delhi, [UGC Major Research Project, F. No. 34-308\2008 (SR) Dated: 31.12.2008 (DD)] for financial support. We also thank the Department of Science and Technology (DST), New Delhi, for providing single-crystal diffractometer facility at the Department of Chemistry, University of Calcutta, through DST–FIST program. We are also thankful to Dr (Mrs.) Krishna Das Saha, Indian Institute of Chemical Biology, for her help on MTT assays. The generous help of Mr. Bijan Pal, Research Scholar, Department of Chemistry, University of Calcutta, India, to determine the DNA binding constant is also duly acknowledged.

References

[1] R. Martinez, L. Chacon-Garcia. *Curr. Med. Chem.*, **12**, 127 (2005).
[2] M. Chauhan, K. Banerjee, F. Arjmand. *Inorg. Chem.*, **46**, 3072 (2007).
[3] J. Chen, X. Wang, Y. Shao, J. Zhu, Y. Zhu, Y. Li, Q. Xu, Z. Guo. *Inorg. Chem.*, **46**, 3306 (2007).
[4] Z.-.H. Xu, F.-.J. Chen, P.-.X. Xi, X.-.H. Liu, Z.-.Z. Zeng. *J. Photochem. Photobiol.*, **196**, 77 (2008).
[5] D.R. Boer, A. Canals, M. Coll. *Dalton Trans.*, **3**, 399 (2009).
[6] R. Palchaudhuri, P.J. Hergenrother. *Curr. Opin. Biotechnol.*, **18**, 497 (2007).
[7] T. Jun, W. Bochua, Z. Liancai. *Bioorg. Med. Chem. Lett.*, **17**, 1197 (2007).

[8] X.-.Y. Wang, J. Zhang, K. Li, N. Jiang, S.-.Y. Chen, H.-.H. Lin, Y. Huang, L.-.J. Maa, X.-.Q. Yua. *Bioorg. Med. Chem.*, **14**, 6745 (2006).
[9] X.-.Y. Yu, S.-.H. Cai, X. Xu, Z. Chen. *Inorg. Chem.*, **44**, 6755 (2005).
[10] A. Neves, H. Terenzi, R. Horner, A. Horn Jr, B. Szpoganicz, J. Sugai. *Inorg. Chem. Commun.*, **4**, 388 (2001).
[11] S. Dhar, M. Nethaji, A.R. Chakravarty. *Dalton Trans.*, 344 (2005).
[12] S. Dhar, D. Senapati, P.K. Das, P. Chattopadhyay, M. Nethaji, A.R. Chakravarty. *J. Am. Chem. Soc.*, **125**, 12118 (2003).
[13] P.U. Maheswari, K. Lappalainen, M. Sfregola, S. Barends, P. Gamez, U. Turpeinen, I. Mutikainen, G.P. van Wezel, J. Reedijk. *Dalton Trans.*, 3676 (2007).
[14] R.R. Gagne, C.L. Spiro, T.J. Smith, C.A. Hamann, W.R. Thies, A.K. Shiemke. *J. Am. Chem. Soc.*, **103**, 4073 (1981).
[15] Z. Otwinowski, W. Minor. In *Methods in Enzymology*, C.W. Carter Jr, R.M. Sweet (Eds), Vol. 276, p. 307, Academic Press, New York (1997).
[16] Bruker, (2000). *SMART, SAINT. Software Reference Manual*, Bruker AXS Inc. Madison, Wisconsin, USA.
[17] G.M. Sheldrick. *Acta Cryst. A*, **64**, 112 (2008).
[18] L.J. Farrugia. *J. Appl. Crystallogr.*, **32**, 837 (1999).
[19] T. Mosmann. *J. Immunol. Methods*, **65**, 55 (1983).
[20] M. Ohno, T. Abe. *J. Immunol. Methods*, **145**, 199 (1991).
[21] A. Banerjee, S. Ganguly, T. Chattopadhyay, K. Banu, A. Patra, S. Bhattacharya, E. Zangrando, D. Das. *Inorg. Chem.*, **48**, 8695 (2009).
[22] T. Chattopadhyay, M. Mukherjee, A. Mondal, P. Maiti, A. Banerjee, K. Banu, S. Bhattacharya, B. Roy, D.J. Chattopadhyay, T.K. Mondal, M. Nethaji, E. Zangrando, D. Das. *Inorg. Chem.*, **49**, 3121 (2010).
[23] N.H. Pilkington, R. Robson. *Aust. J. Chem.*, **23**, 2225 (1970).
[24] D.C. Carter, J.X. Ho. *Adv. Protein Chem.*, **45**, 177 (1994).
[25] C. Marzano, M. Pellei, D. Colavito, S. Alidori, G.G. Lobbia, V. Gandin, F. Tisato, C. Santini. *J. Med. Chem.*, **25**, 7317 (2006).